

Final Version, November 19, 2001

Recent developments in the characterization of superconducting films by microwaves

M.A. Hein^a, M. Getta^a, S. Kreiskott^a, B. Mönter^a, H. Pief^a, D.E.Oates^b, P.J. Hirst^c, R.G. Humphreys^c, H.N. Lee^d, S.H. Moon^d

^a Dept. of Physics, University of Wuppertal, Germany, ^b MIT Lincoln Laboratory, Lexington, MA, U.S.A., ^c QinetiQ, Malvern, U.K., ^d LG Electronics Inc., Seoul, Korea.

Abstract: We describe and analyze selected surface impedance data recently obtained by different groups on cuprate, ruthenate and diboride superconducting films on metallic and dielectric substrates for fundamental studies and microwave applications. The discussion includes a first review of microwave data on MgB₂, the weak-link behaviour of RABiTS-type YBa₂Cu₃O_{7- δ} tapes, and the observation of a strong anomalous power-dependence of the microwave losses in MgO at low temperatures. We demonstrate how microwave measurements can be used to investigate electronic, magnetic, and dielectric dissipation and relaxation in the films and substrates. The impact of such studies reaches from the extraction of microscopic information to the engineering of materials and further on to applications in power systems and communication technology.

Keywords: Surface impedance, superconducting films, microwave dissipation, relaxation.

Address: Dr. Matthias Hein, Dept. of Physics, Univ. of Wuppertal, D-42097 Wuppertal, Germany. Tel. +49(202)439-2747, Fax +49(202)439-2811
Email: mhein@venus.physik.uni-wuppertal.de

1. Microwave measurements in condensed matter physics

1.1 Theoretical background

This paper illustrates the relevance of microwave measurements for the investigation of electronic and magnetic transport and ordering in condensed matter. While most work has been done on solids, the described techniques could also be adapted to soft matter or liquids. The presentation is based on a selection of examples and does not attempt to provide a complete description of activities in this field.

The complex-valued surface impedance $Z_s=R_s+iX_s$ at a microwave frequency $\omega=2\pi f$ is related to the permeability and conductivity of a material, \mathbf{m} and \mathbf{s} , in the local limit by

$$Z_s = R_s + iX_s = \sqrt{i\omega \frac{\mathbf{m}(\omega)}{\mathbf{s}(\omega)}}, \quad (1)$$

where R_s and X_s are the surface resistance and reactance [1]. The material parameters \mathbf{m} and \mathbf{s} are complex-valued and frequency dependent, e.g., via electronic, magnetic, or dielectric relaxation. The generalized conductivity \mathbf{s} characterizes electrical conduction through transport and displacement currents.

The electrodynamic response of *metallic materials* provides information on the electronic properties within a surface layer of the order of the London penetration depth ~ 200 nm, and on a variable time scale $\sim 1/\omega$. Such information is complementary to thermodynamic bulk properties and low-frequency transport data. The high frequencies also help to derive Fermi surface properties, which would require strong magnetic fields at very low temperatures otherwise [2]. We will focus in the following on *superconductors*, for which Z_s bears information on the density of states and quasiparticle excitations above and below the transition temperature T_c [3]. It is also related to the phase purity, grain connectivity and interface effects of technical materials, which cannot readily be studied at similar resolution by

other techniques [4,5]. Such information is required for optimizing epitaxial films or biaxially textured tapes in terms of critical current density, low loss, and power handling.

Similarly, studies of microwave dissipation and relaxation in *magnetic* or *dielectric* materials have received great attention recently, e.g., to resolve the coupling of spins and charges in magnetic superconductors like the borocarbides or rutheno-cuprates [6,7,8], or materials displaying colossal magneto-resistance [9], or to search for low-loss ferrite or ferroelectric materials for frequency-agile devices [10,11,12].

1.2 Brief history of microwave superconductivity

A historical success of microwave measurements was achieved by H. London, when he studied Sn [13]. His investigations led to the first direct experimental determination of the superconducting energy gap, the development of the two-fluid model, and the analysis of the anomalous skin effect [14,15]. Later on, Pippard exploited the information contained in the microwave measurements of noble metals to clarify the Fermi surface of copper [14], and to develop a comprehensive theory of electronic transport in solids [2].

More recently, the characterization of the hole-doped cuprate superconductors revealed a power-law temperature dependence of the quasiparticle fraction at low temperatures, which helped establish the d-wave symmetry of the order parameter [16]. Part of the ongoing work focuses on the high residual R_s -values in $\text{Bi}_2\text{Sr}_2\text{CaCu}_2\text{O}_{8+y}$, which are difficult to explain merely by gap nodes. Non-quasiparticle s -contributions from, e.g., charge density waves in the inherently inhomogeneous cuprates have been suggested [17], which would modify our understanding of electronic transport in these materials. Other microwave studies aim at resolving the symmetry of the order parameter in the electron-doped cuprates [18]. Comparative measurements on $\text{R}_{2-x}\text{Ce}_x\text{CuO}_{4-\delta}$ (R=Pr,Nd) indicated power-law behaviour of $\Delta I(T)$,

in accordance with phase-sensitive experiments pointing to d-wave symmetry [19], but in contradiction to tunneling data [20].

The first microwave measurements on the spin-triplet superconductor Sr_2RuO_4 at 10 GHz were reported very recently [21]. This material, though isostructural with $\text{La}_{2-x}\text{Sr}_x\text{CuO}_4$ [22], displays the maximum $T_c \sim 1.5\text{K}$ in the undoped state. Reflecting the high purity of this material, the surface impedance revealed strong quasiparticle relaxation, $\omega\tau \sim 1$, throughout the superconducting state. Such measurements are, beside their relevance to resolve the pair state in the ruthenates, of great general interest since the involved energy scales for frequency, temperature, relaxation and pairing are all comparable.

MgB_2 is another novel superconductor of great interest, due to its high T_c and possible applications [23]. Beside polycrystalline pellets and wires, thin films have become available for extended microwave studies (see [24,25] and Sec. 3.1).

At present at least 50 renowned academic and industrial groups study superconductors at microwave frequencies, to about equal parts for fundamental and applied physics. While the future development of this discipline depends on available funding, exciting results can be expected in the near term, both for broadened understanding of superconductivity and applications optimizing our social and economic resources.

2. Microwave measurements for the characterization of thin films

Conceptually, the surface impedance describes the propagation of electromagnetic waves across the interface between vacuum and matter. Eq.(1) implies bulk properties, when the thickness of the material extends over many penetration lengths, $t \gg \lambda$. New aspects arise for $t < \lambda$, due to partial reflection and transmission at the additional film-substrate interface, e.g., in very thin films or near T_c . The effective surface impedance follows from an implicit equation [5,26,27]:

$$Z_{eff}(t) = Z_{s\infty} \times \frac{Z_{s\infty} \times \tanh(\mathbf{b}t) + Z_{sub}}{Z_{s\infty} + Z_{sub} \times \tanh(\mathbf{b}t)}, \quad (2)$$

where $Z_{s\infty}$ is the bulk value, $\mathbf{b} = i\omega\mu/Z_{s\infty}$ the propagation constant, and Z_{sub} the surface impedance of the substrate.

Eq. (2) can be solved approximately, e.g., for a superconducting film of thickness t_S on a lossless dielectric, leading to $Z_{eff}(t_S) \sim Z_{s\infty} \times \coth(\mathbf{k}t_S)$, where \mathbf{k} is the inverse skin (penetration) depth above (below) T_c . Another interesting case is a normal conducting cap layer of thickness t_N and resistivity \mathbf{r}_N on a superconducting film. The propagation of the wave through the cap layer into the superconductor, or vice versa, enhances $R_{s\infty}$ in proportion to t_N , namely by $X_{s\infty}^2 \times t_N / \mathbf{r}_N$ or $X_{s\infty}^2 \times t_N / \mathbf{r}_N \times (I/t_S)^2$, respectively. The explicit I -dependence in the latter case has been used to extract absolute I -values [28].

Eq. (2) becomes more complicated for multilayers, like a superconducting film on a metallic substrate with dielectric buffer. The effective reactance of the buffer can become comparable with the reactance of the superconductor and the resistance of the metal. Numerical techniques and reference measurements are then required to determine $Z_{s\infty}$.

The principle benefit of Z_s measurements for the characterization of thin films is increased by technological considerations. Thin films are often much more relevant for applications than bulk material, in terms of fabrication, refrigeration and power consumption. Thin films are also preferable for highly anisotropic materials like the cuprates, or for materials prepared by vapor diffusion like Nb_3Sn [5] or MgB_2 [24]. Should the preparation of single-crystals be complicated by an unfavorable thermodynamic phase diagram, thin films may allow to evaluate intrinsic properties. Alternatively, comparative measurements of poly- and single-crystalline bulk and thin film samples are beneficial to study the impact of defects like grain boundaries, interfaces or impurities [5,29,30].

Z_{eff} -measurements also provide information on the electrodynamics of the substrate. For instance, the strongly temperature dependent permittivity of SrTiO_3 leads to oscillations of $Z_{\text{eff}}(T)$ [26]. Present efforts aim at understanding the different microwave properties of bulk and thin film SrTiO_3 for device applications. Another example is the observation of dielectric relaxation in LaAlO_3 or MgO , which cause non-monotonic temperature and field dependences of the loss tangent and hence the quality factor of microwave devices [31-33].

3. Recent developments of the microwave characterization of superconductors

3.1 The surface impedance of MgB_2

Many groups have been investigating the microwave properties of MgB_2 during various stages of material optimization [24,25,34-38]. Fig. 1 compares our first $R_{\text{eff}}(T)$ -data of a polycrystalline 400nm-thick MgB_2 film on sapphire with three other superconductors at 87 GHz. The lowest R_s -values in the entire T -range are observed for Nb_3Sn , due to its large, almost isotropic energy gap and its low normal-state resistivity. Epitaxial $\text{YBa}_2\text{Cu}_3\text{O}_{7-\delta}$ (YBCO) displays the second lowest losses for $T < T_c$, but the large resistivity causes significant corrections of $R_{\text{eff}}(T > T_c)$. The MgB_2 film displays a low $R_{\text{eff}} = 0.49 \Omega$ in the normal state, which corresponds to a resistivity of $r \sim 20 \mu\Omega\text{cm}$. The broad transition indicates inhomogeneous film properties, but the residual resistance is promisingly low. This becomes clearer from Fig. 2, which summarizes $R_s(f)$ -data of MgB_2 at three selected temperatures. The temperature dependence of R_{eff} below about 30 K is consistent with a reduced energy gap ~ 0.8 , in accordance with other RF studies [37,39].

The scatter of the $R_s(f)$ -data in Fig. 2 reflects the variability of the quality of bulk samples and films, which is not yet intrinsic. Only the lowest R_{eff} -values at 4.2 and 20 K scale almost like f^a with $a \sim 2$, as expected for a phase-pure superconductor below the gap frequency. The R_s -values are well below those of granular YBCO, and already close to

epitaxial YBCO at 77 K [5]. The frequency exponent decreases towards $a \sim 1$ for lower sample quality and higher temperatures, indicating the growing influence of normal or weakly superconducting material. The high value of $R_{\text{eff}}(30\text{K})$ at 87 GHz could indicate, besides inhomogeneities, the existence of a small gap value.

3.2 The surface impedance of YBCO on RABiTS

Microwave measurements of YBCO on rolling-assisted biaxially-textured substrates (RABiTS) [40] are helpful to optimize the grain boundary coupling and phase purity. Fig. 1 shows $R_{\text{eff}}(T)$ of a 400nm-thick YBCO film on a 340nm-thick $\text{CeO}_2/\text{YSZ}/\text{CeO}_2$ trilayer on textured Ni [41]. While the low normal-state resistance is related to the low impedance of the thin buffer and the metallic substrate, the high R_s -level in the superconducting state is attributed to low- and large-angle grain boundaries or microcracks [5,42-44]. These effects add not only to the total surface resistance but lead also to a larger thickness correction due to an enhanced penetration length.

Fig. 3 illustrates the influence of weak grain boundary coupling, by relating R_{eff} to the critical current density. The scaling $R_{\text{eff}}(77\text{K}) \propto J_c^{-1/2}$ for all types of YBCO is reminiscent of Josephson coupling or quasiparticle tunneling at grain boundaries. This result is in contrast with the recent findings for epitaxial films [43], probably indicating the different microstructure of the two types of samples. At 4.2 K, the losses remain on a much higher level in the RABiTS samples than in epitaxial films. The different scaling at low and high temperatures is emphasized by the similarity of $R_{\text{eff}}(77\text{K})$ and the difference $R_{\text{eff}}(77\text{K}) - R_{\text{eff}}(4.2\text{K})$. Our results illustrate that high-frequency measurements are more sensitive to defects than low-frequency techniques, which essentially map critical current densities.

3.3 The nonlinear surface impedance of superconductors on MgO

Understanding the nonlinearities in microwave devices is relevant for applications in communication systems [45]. We have therefore studied microwave losses and intermodulation distortion (IMD) of epitaxial YBCO films on MgO using stripline resonators [33,45]. The total surface resistance contains contributions from the superconductor and the dielectric, $R_{\text{tot}}=R_s+G\tan\delta$, where G is a geometry factor. Changes of the reactance are similarly composed of changes of the penetration depth and dielectric permittivity.

Fig. 4 compares the power dependent R_{tot} for YBCO and Nb, which display very similar behaviour. We conclude that R_{tot} is dominated by power dissipation in the dielectric and the superconductor at low and high power, respectively, which is in accordance with the linear and quadratic frequency dependences of R_{tot} measured in the two power ranges. Using $R_s\sim 2\ \mu\Omega$, which is typical for YBCO at 2.3 GHz and 1.7 K [5], and $R_{\text{tot}}\sim 20\ \mu\Omega$, we derive $\tan\delta\sim 3\times 10^{-5}$, which is 1-2 orders of magnitude higher than expected for MgO at 20 K [46,47].

Fig. 5 relates R_{tot} of the YBCO sample to ΔX_{tot} and the IMD signal at 5 K and 2.3 GHz. R_{tot} passes through a minimum at -20 dBm, while X_{tot} remains constant, at least up to -30 dBm. The increase of R_{tot} and X_{tot} at high power is attributed to the nonlinear response of the superconductor [5]. The IMD signal at low power displays approximately the expected cubic power dependence [48], passes through a plateau in the region where R_{tot} decreases, and rises again more steeply where R_{tot} and X_{tot} increase. The correlation between R_{tot} and the IMD product reveals the dissipative nature and a fast response time of the anomaly.

We were able to model the behaviour by defect dipole relaxation in MgO [33,49]. Our data imply $\omega t_d < 1$ and a electric field-dependence of the dielectric relaxation time t_d on a scale of $E_0\sim 100$ V/m at $T < 5$ K. This value increased to ~ 30 kV/m at 20 K, reflecting the growing

influence of the superconducting nonlinearity, which eventually masked the dielectric anomaly at elevated temperatures.

4. Conclusions

We have illustrated the benefit of surface impedance measurements for the characterization of cuprate, ruthenate and diboride superconducting films on metallic and dielectric substrates for fundamental studies and applications by selected examples. The high frequencies make this technique sensitive to electronic, magnetic, or dielectric dissipation and relaxation in the films and substrates.

The temperature and frequency dependent surface resistance of polycrystalline MgB_2 , while presently limited by the quality of the available material, is already comparable to that of optimized epitaxial YBCO films, hence opening great potential for applications.

The surface resistance of biaxially textured YBCO films on buffered Ni reveals strong limitations from weak Josephson coupling across grain boundaries or microcracks. Due to the high sensitivity of microwave measurements, R_s -guided optimization of superconducting RABiTS tapes is expected to facilitate further development towards conductors with high engineering critical current densities.

The temperature and power dependent surface resistance of superconducting films on MgO displayed pronounced anomalies, which are associated with defect dipole relaxation in the substrate. The nonlinear loss tangent of MgO is relevant for any microwave device application involving this dielectric.

Acknowledgments

We thank S.Y. Lee, S. Ohshima, and T.C. Shields for providing R_s data on MgB_2 and YBCO prior to publication, and J. Derov, J. Halbritter, P. Lahl, N. Newman, S.H. Park, A.

Velichko, and R. Wördenweber for helpful discussion. This work has been funded in part by the EPSRC and MOD (UK), and AFOSR (U.S.A.). Part of this material is based upon work supported by the European Office of Aerospace Research and Development, AFOSR/AFRL, under Contract F61775-01-WE033.

References

- [1] J.D. Jackson: Classical electrodynamics (deGruyter, Berlin, 1983).
- [2] C. Kittel: Introduction to Solid State Physics (Wiley, New York, 1968).
- [3] J.R. Waldram: Superconductivity of metals and cuprates (IOP, Bristol, 1996).
- [4] A.M. Portis: Electrodynamics of high-temperature superconductors, Lecture Notes in Physics, Vol. 48 (World Scientific, Singapore, 1993).
- [5] M.A. Hein: High-temperature superconductor thin films at microwave frequencies, Springer Tracts of Modern Physics, Vol. 155 (Springer, Heidelberg, 1999).
- [6] A. Andreone et al., Physica C**319** (1999) 141.
- [7] D.P. Choudhury, H. Srikanth, S. Sridhar, P.C. Canfield, Phys. Rev. **B58** (1998) 14490.
- [8] M. Pozek, A. Dulcic, D. Paar, G.V.M. Williams, S. Krämer, Phys. Rev. **B64** (2001) 064508.
- [9] S.E. Lofland, S.M. Bhagat, S.D. Tyagi, Y.M. Mukovskii, S.G. Karabashev, A.M. Balbashov, J. Appl. Phys. **80** (1996) 3592.
- [10] D.E. Oates, G.F. Dionne, IEEE Trans. Appl. Supercond. **9** (1999) 4170.
- [11] O.G. Vendik, L.T. Ter-Martirosyan, S.P. Zubko, J. Appl. Phys. **84** (1998) 993.
- [12] D.E. Steinhauer et al., Appl. Phys. Lett. **75** (1999) 3180.
- [13] H. London, Proc. Roy. Soc. **A176** (1940) 522.
- [14] A.B. Pippard, Rep. Prog. Phys. **23** (1960) 176.
- [15] G.E.H. Reuter, E.H. Sondheimer, Proc. Roy. Soc. **195** (1948) 336.
- [16] W.N. Hardy et al., Phys. Rev. Lett. **70**, (1993) 3999; A. Hosseini et al., Phys. Rev. **B60** (1999) 1349.
- [17] S. Sridhar, Z. Zhai, Physica C**341-348** (2000) 2057.

- [18] J.D. Kokales et al., Phys. Rev. Lett. **85** (2000) 3696.
- [19] C.C. Tsuei, J.R. Kirtley, Phys. Rev. Lett. **85** (2000) 182.
- [20] L. Alff et al., Phys. Rev. Lett. **83** (1999) 2644.
- [21] M. Hein, R.J. Ormeno, C.E. Gough, J. Phys.: Condens. Matter **13** (2001) L65.
- [22] Y. Maeno et al., Nature **372** (1994) 532.
- [23] J. Nagamatsu, N. Nakagawa, T. Muranaka, Y. Zenitani, J. Akimitsu, Nature **410** (2001) 63.
- [24] N. Hakim et al., Appl. Phys. Lett. **78** (2001) 4160.
- [25] S.Y. Lee et al., cond-mat/0105327.
- [26] N. Klein et al., J. Appl. Phys. **67** (1990) 6940.
- [27] M.J. Lancaster: Passive microwave device applications of high-temperature superconductors (Cambridge University Press, Cambridge, 1997).
- [28] A.G. Zaitsev et al., IEEE Trans. Appl. Supercond. **11** (2001) 3423; A. G. Zaitsev et al., another contribution to this conference.
- [29] S. Hensen, G. Müller, C.T. Rieck, K. Scharnberg, Phys. Rev. **B56** (1997) 6237.
- [30] M.A. Hein, T. Kaiser, G. Müller, Phys. Rev. **B61** (2000) 640.
- [31] C. Zuccaro, M. Winter, N. Klein, K. Urban, J. Appl. Phys. **82** (1997) 5695.
- [32] B.A. Aminov et al., IEEE Trans. Appl. Supercond. **9** (1999) 4185.
- [33] M.A. Hein et al, subm. to Appl. Phys. Lett. (2001), cond-mat/0108346.
- [34] A.A. Zhukov et al., Supercond. Sci. Technol. **14** (2001) L13.
- [35] Yu.A. Nefyodov et al., cond-mat/0107057.
- [36] A.A. Zhukov et al., cond-mat/0107240v2.
- [37] N. Klein et al., cond-mat/0107259.

- [38] C.E. Gough, R.J. Ormeno, A. Sibley, M. Hein, S. NishiZaki, Y. Maeno, *subm. to Physica C* (2001).
- [39] F. Manzano and A. Carrington, *cond-mat/0106166*.
- [40] A. Goyal et al., *Appl. Supercond.* **4** (1998) 403.
- [41] S. Kreiskott, U. Wuppertal, unpublished.
- [42] J. Halbritter, *J. Appl. Phys.* **68** (1990) 6315; **71** (1992) 339.
- [43] S. Ohshima et al., *IEEE Trans. Appl. Supercond.* **11** (2001) 3493; S. Ohshima et al., another contribution to this conference.
- [44] G. Kästner et al., *Supercond. Sci. Technol.* **12** (1999) 366.
- [45] D.E. Oates et al., another contribution to this conference.
- [46] J. Krupka, R.G. Geyer, M. Kuhn, J.H. Hinken, *IEEE Trans. Microwave Theory Tech.* **42** (1994) 1886.
- [47] T. Konaka, M. Sato, H. Asano, S. Kubo, *J. Supercond.* **4** (1991) 283.
- [48] T. Dahm, D.J. Scalapino, *J. Appl. Phys.* **81** (1997) 2002; *Phys. Rev.* **B60** (1999) 13125.
- [49] V.V. Daniel: *Dielectric Relaxation* (Academic Press, New York, 1967).

Figure captions

Fig. 1. Temperature dependent surface resistance of epitaxial YBCO on LaAlO_3 (black dotted curves), polycrystalline Nb_3Sn on sapphire (grey dotted), biaxially textured YBCO on buffered Ni (dashed), and polycrystalline MgB_2 on sapphire (solid). The thick (thin) curves denote effective data (corrected for film thickness).

Fig. 2. Frequency dependent R_{eff} of bulk (small black symbols) and thin film MgB_2 (large grey) at 4.2 K (solid squares), 20 K (hatched), and 30 K (shaded), collected from [24,25,34-38] and unpublished sources. The grey dotted line represents $R_s(77\text{K})$ of epitaxial $\text{YBa}_2\text{Cu}_3\text{O}_{7-\delta}$ films [5].

Fig. 3. Correlation between R_{eff} of biaxially textured YBCO films on Ni at 4.2 K (solid squares) and 77 K (shaded) and $R_{\text{eff}}(77) - R_{\text{eff}}(4.2)$ (hatched) and the critical current density at 77 K. The dotted line denotes $R_{\text{eff}} \propto J_c^{-1/2}$. Data on electrophoretic YBCO films on Ag and epitaxial films on LaAlO_3 [5] are shown for comparison.

Fig. 4. Power dependent R_{tot} for a YBCO (diamonds) and a Nb film (triangles) on MgO [33]. Absolute R_{tot} -values were 8.5 and 12 $\mu\Omega$ at 5 K, and 19 $\mu\Omega$ for both samples at 1.7 K.

Fig. 5. Correlation between R_{tot} of the YBCO film of Fig. 4 (circles), total reactance (triangles) and IMD product (squares) [33].

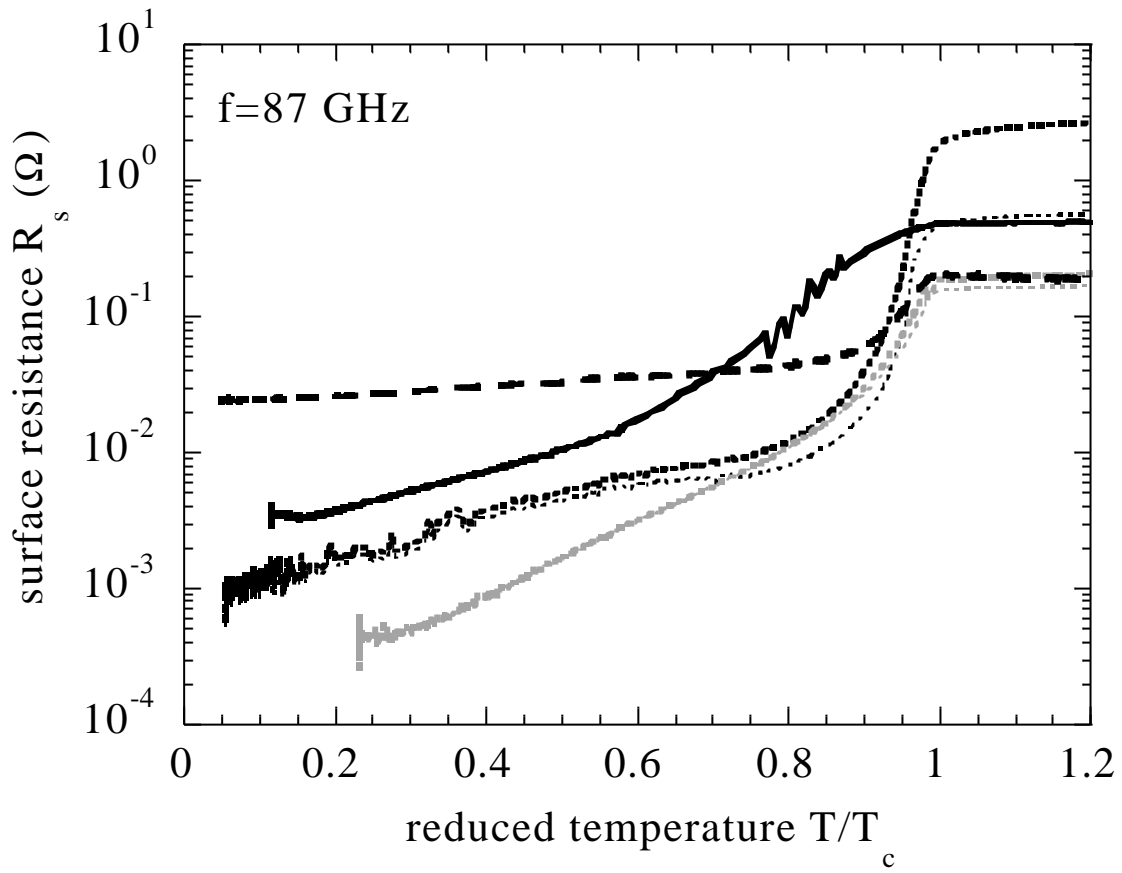


Fig. 1, Hein et al., paper B3-01.

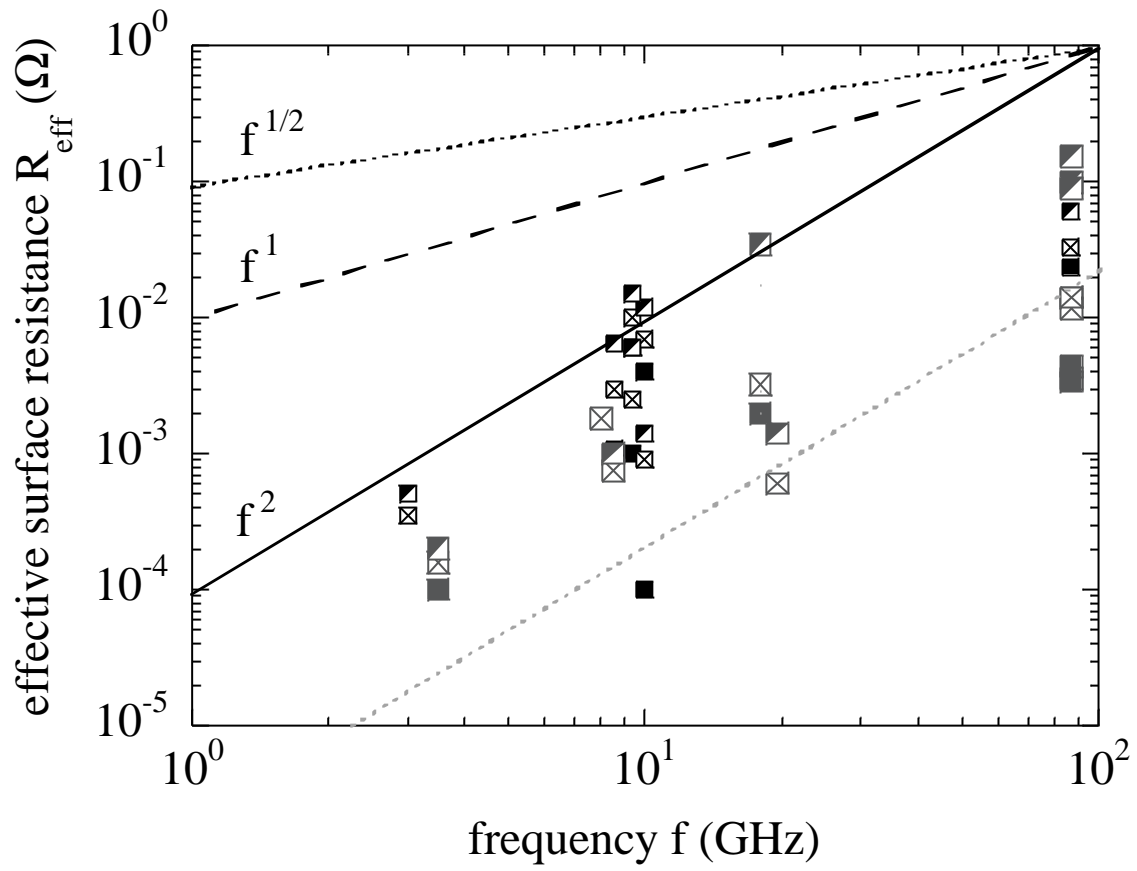


Fig. 2, Hein et al, paper B3-01.

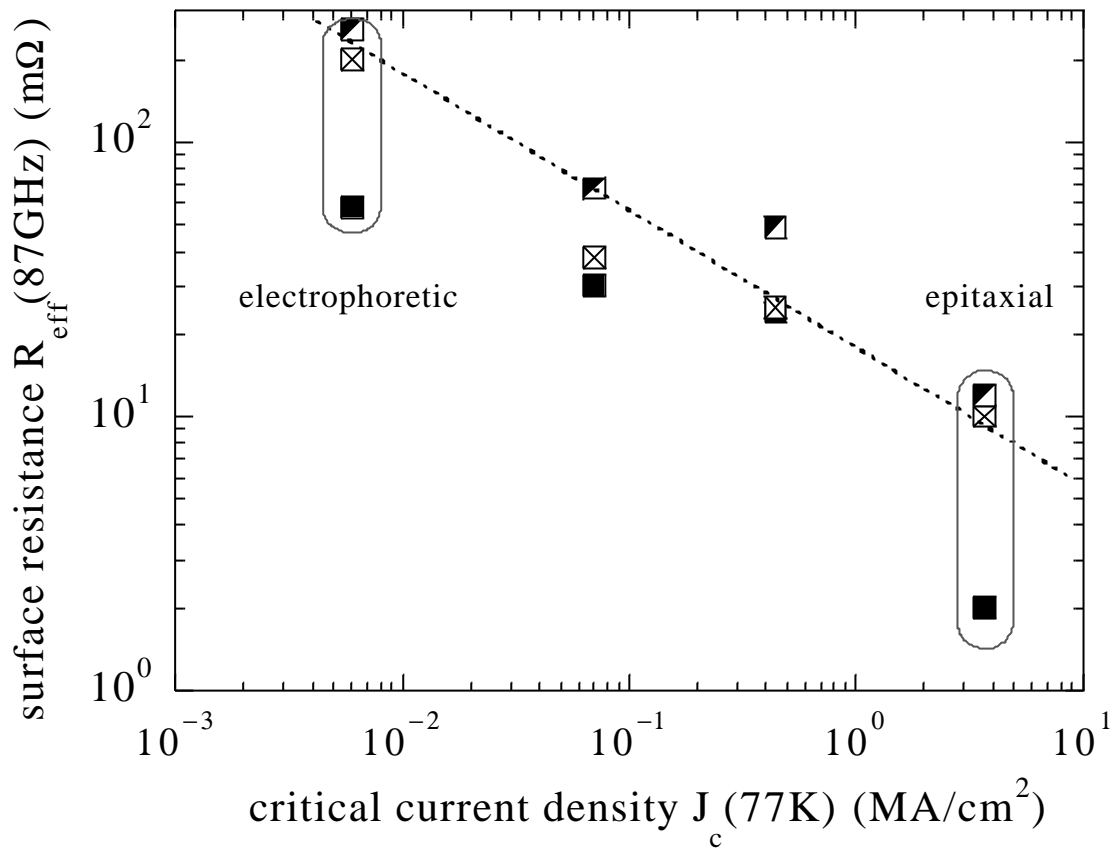


Fig. 3, Hein et al., paper B3-01.

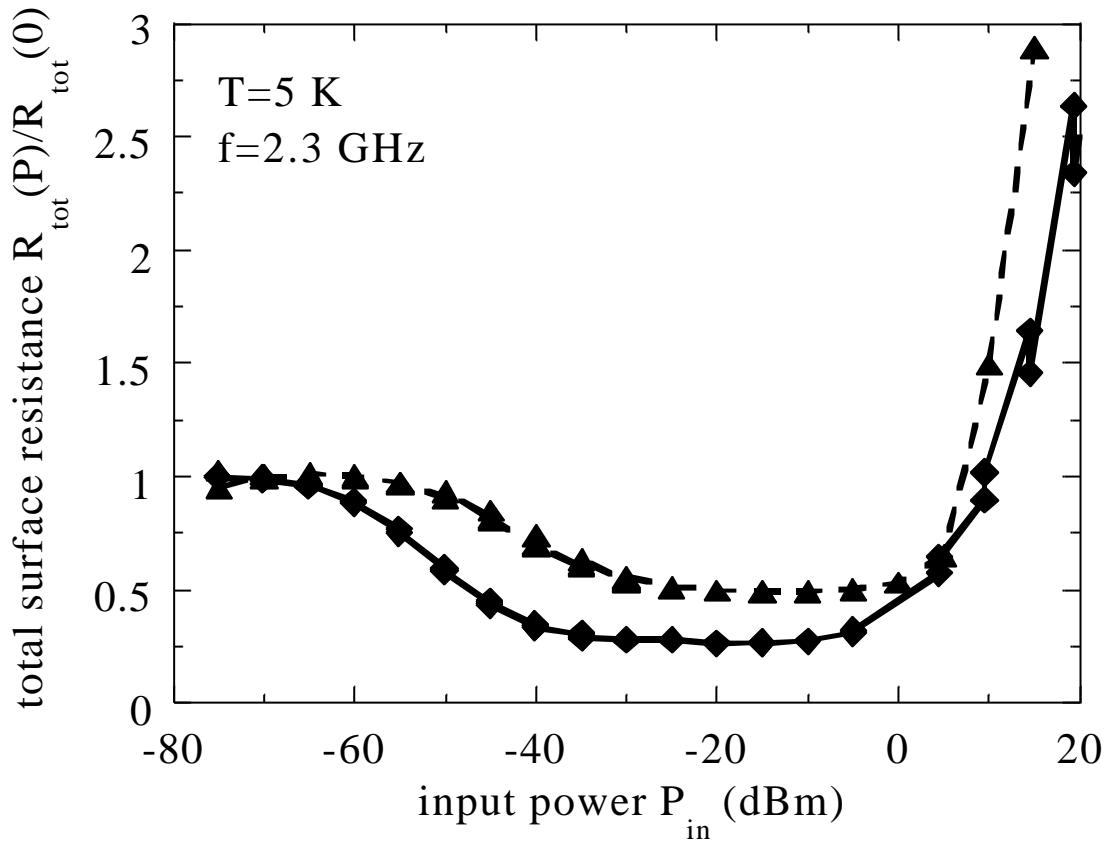


Fig. 4, Hein et al., paper B3-01.

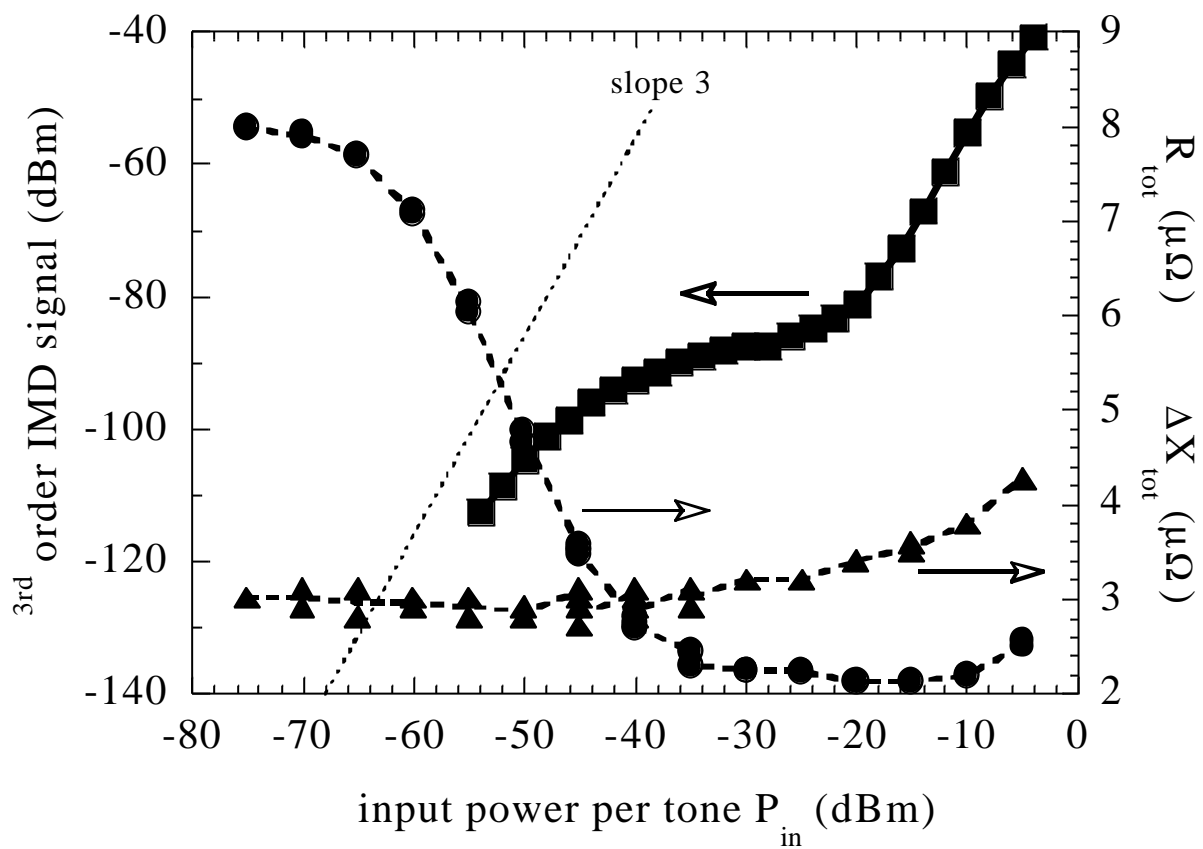


Fig. 5, Hein et al., paper B3-01.